Available online at www.sciencedirect.com
ScienceDirect
International Journal of Solids and Structures 45 (2008) 879–893
INTERNATIONAL JOURNAL OF SOLIDS AND STRUCTURES
www.elsevier.com/locate/ijsolstr

Conductance of rough random profiles

M. Ciavarella *, S. Dibello, G. Demelio

Politecnico di Bari, V.le Japigia 182, Bari 70125, Italy

Received 19 May 2005; received in revised form 1 September 2007
Available online 19 September 2007

Abstract

Recently, the real contact area and the compliance and electrical resistance for a rough surface defined with a Weierstrass series have been studied under the assumption that superposed self-affine sine waves had well separated wavelengths, extending the celebrated procedures pioneered by Archard [Archard, J.F., 1957. Elastic deformation and the laws of friction. Proc. R. Soc. Lond. A 243, 190–205]. Here, more realistic fractal rough surface profiles are considered, by using the Weierstrass series with random phases, and with much lower separation of the various scales, using a full or a hybrid numerical/analytical technique. A non-linear layer algorithm is developed which is a very efficient approximate tool to study this problem, avoiding the need for averaging over various realizations of profiles with random phases. The multiscale problem is solved by a cascade of 2-scales problems, each of which is solved with a few elements for an imposed contact area, deriving load as a function of indentation and the conductance by differentiation using Barber's analogy theorem.

Dimensionless results for the conductance as a function of applied pressures show that the conductance seems to be close to a power law at low loads, and is nearly linear at intermediate loads (following the normalized single sinusoidal case except at the origin). At high loads, the conductance becomes strongly dependent on fractal dimension because of weak dependence on the contribution of small wavelength scales (higher order terms in the series). Since roughness tends to be squeezed out, the conductance tends to increase more than linearly (more so, the smaller is the fractal dimension). However, another limit could be found in terms of the finite size of the specimen, which may suggest reaching a finite limit. The resulting curves could then be sigmoidal, as confirmed by qualitative comparisons with experiments in the literature.

Keywords: Electrical contact; Electrical resistance; Roughness; Rough contact

1. Introduction: elastic contact of rough random surfaces

Various statistical (Greenwood and Williamson, 1966; Whitehouse and Archard, 1970; Bush et al., 1975) and fractal theories (Archard, 1957; Majumdar and Bhushan, 1991; Ciavarella et al., 2000) have attempted to solve the problem of mechanical contact of rough surfaces. Recent theories agree that the elastic contact area is shown to go to zero in the limit of fractals when all the wavelengths are included. In particular, Ciavarella et al. (2000) show that the contact area at large enough resolutions tends to have a fractal dimension of $2D$, where D is the dimension of the profile.

* Corresponding author.
E-mail address: mciava@poliba.it (M. Ciavarella).

0020-7683/$ - see front matter © 2007 Elsevier Ltd. All rights reserved.
doi:10.1016/j.ijsolstr.2007.09.009

It is well known (and common experimental observation) that contact does not happen on the nominal area but on a great number of contact spots of various forms and dimensions, that depend on the highest dimension of the profile, distributed on nominal contact area. Actually, according to the results of he contact area can then be considered is itself a fractal, and in the Mandelbrot's terminology (Mandelbrot, 1982) it is a lacunar fractal, i.e. it has fractal dimension less than the topological dimension, as opposed to invasive fractals, which have the opposite property.

The "structure" of the fractal is similar to a Cantor set. This raises a question over the limit conductance in a "zero" contact area (is it also zero or finite?) i.e. as found within the assumption of elasticity theory applied to fractal surfaces contact mechanics. If the contact conductance is found to be zero for these models, then maybe plastic deformation or other small scale processes need to be considered to find a realistic value; if on the contrary, it is finite, maybe this is close to the true value. Work in progress by some colleagues (Manners and Gholami, 2005) is showing that if contact sizes are progressively reduced to zero, and the pattern of gaps and contacts remains uniform so that the gap sizes also tend to zero, then the resistance will tend to *zero i.e. the conductance to infinity*! However, if the contacts are arranged in the pattern generated by the 'Cantor Dust' model, so that the gaps remain finite, then the *resistance remains finite*. More generally, where the contact area is progressively reduced on a sequence of scales, then the resistance is the sum of a series of values appropriate to each scale. The resulting series converges to a finite limit for sequences that seem reasonable for typical surfaces and mechanical contact processes, but can diverge if the contact area scales down fast enough, so we can even have the other limit of infinite resistance, *i.e. zero conductance*!

Experimental data on electrical conductance under similar conditions seem surprisingly different by various orders of magnitude, and moreover seem to follow different trends both quantitatively and qualitatively (see Fig. 1). This may be partly due to the effect of films and oxides, which vary largely between one surface and another (not all mechanical contact spot conduct, but only the so-called "a-spot" according to Holm, 1958). However, it appears that the rms roughness of the experimental data has a profound effect, as well as possibly other features of roughness which vary between one surface and the other (for example, correlation length), and which are perhaps not captured in standard models.

Despite Fig. 1 indicates a very wide possibilities of laws (in particular, since the plot is log–log, power–laws do not seem to be appropriate in many cases), all existing theories and experimental data on conductance predict power–law effect of load on conductance, i.e.

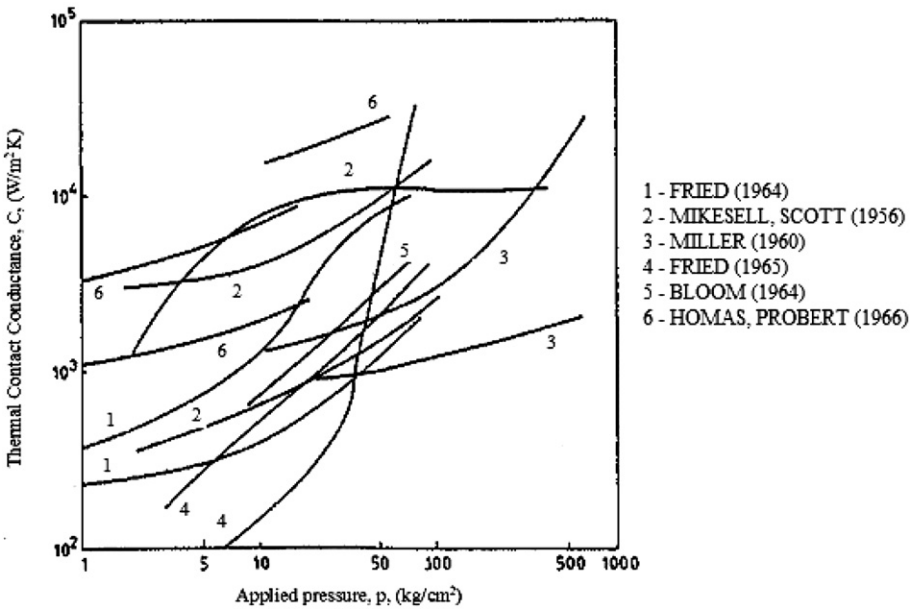

Fig. 1. Contact conductance of stainless steel – stainless steel contacts against applied pressure (adapted from Snaith et al., 1983 and see references therein).

Table 1
A few theories of thermal conductance, and their predicted exponent of the relationship $C = P^m$

Reference	m	Reference	m
Laming (1961)	0.5	Tien (1968)	0.85
Fletcher and Gyorog (1971)	0.56	Thomas and Probert (1970)	0.92
Mal'kov (1970)	0.66	Mikic (1974)	0.94
		Yovanovich (1982)	0.95
		Antonetti (1993)	0.95
		Copper et al. (1969)	0.99

$$C = kP^m \tag{1}$$

where m is an exponent generally either in the range of 0.5 or in the range near 1 (see Table 1 and reference therein, which are thermal conductance theories rather than electrical; however, the two are expected to lead to similar physics).

In particular, the laws of conductance cited in Table 1 are in two significantly different classes. Most theories showing m around 0.5 suppose plastic regime (since the conductance is proportional to the contact radius, whereas the area in the plastic regime grows with P/H, where H is hardness). The second class of theories are those suggesting m closer to 1 and are based on mainly elastic behavior with roughness as it can be shown by one of the earlier theory of rough contact, that of Greenwood and Williamson in the exponential distribution of asperities. If there was no roughness, Hertz theory would predict contact radius and hence conductance growing with power 1/3 of the load for point contact and 1/2 for line contact. As it is clear from Fig. 1 however, the typical conductance laws with perhaps one or two exceptions, seem to indicate various "regimes" rather than a single linear or a power law (in the log–log plot a power–law being a straight line), and because the x–y scales are in the same proportion, it is immediate to see that most curves start from well below linearity (45°), and in most cases increase the power towards sometimes well above the linear regime. In some cases, curves are also turning the other way around (i.e. decreasing the slope), or have even sinusoidal shapes. In some cases, some curves start from linear. Surprisingly, no other conductance other than power–law has emerged so far (at least not in the best of the authors' knowledge) in the literature. In theory, any contact should start from a single contact at the lowest asperity scale (and then, with power 1/3 or 1/2) and then deviate towards the regime dictated by the roughness and the progressive influence of larger and larger scales. A first suggestion will emerge here with a semi-analytical calculation on fractal profiles (although limited to line contact i.e. to the contact of two-dimensional profiles, a somewhat idealized case).

The linearity of the conductance law in the Greenwood–Williamson model can be derived directly. However, to show this here, it is convenient to introduce Barber's analogy in the elastic regime (Barber, 2003), which will be used extensively in the paper when dealing with the roughness. Shortly, Barber makes use of the analogy between the Green's functions of the electrical and mechanical problem on the half-space, together with other theorems in contact mechanics suggesting monotonic force-indentation curve, and derivative, to show that *the conductance of a rough contact is the derivative of the force-indentation curve (incremental stiffness)*,

$$C = -\frac{2}{\rho E}\frac{\partial P}{\partial d} \tag{2}$$

where

$$\frac{1}{E} = \frac{1-\nu_1^2}{E_1} + \frac{1-\nu_2^2}{E_2}, \quad \rho = \rho_1 + \rho_2 \tag{3}$$

are combined elastic modulus and combined resistivities of the materials, E is Young's modulus, and ν is the Poisson's ratio, and P is load at the given separation d, which is equal and opposite to the indentation δ, hence the minus sign in (2).

The analogy also permits to show bounds on conductance for a given finite amplitude of roughness (see Fig. 2). In particular, for a given load at any level, we do not know the exact displacement, but we know the lower and upper values. Hence, we also know bounds on the derivative. For example, the line CA defines the lowest value of the slope at the level of load defined by point A, whereas the line AD defines the highest

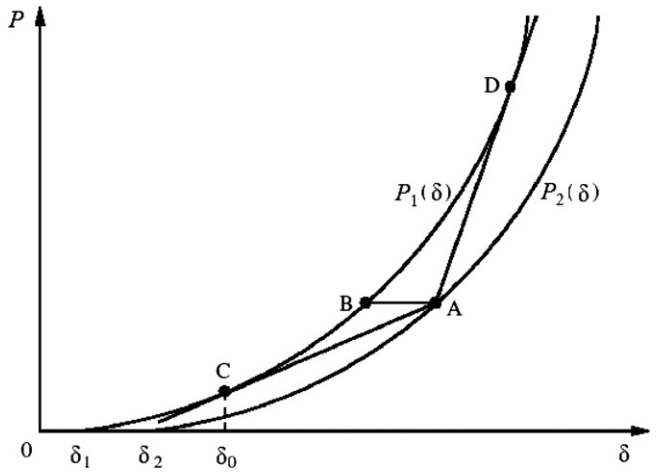

Fig. 2. The load–displacement relation for rough surface must lie between these two curves according to Barber's theorem (Barber, 2003).

value of the slope at the level of load AB, and this way we can construct two bounds on conductance for any given load.

As a consequence, the conductance cannot be infinite even for fractal rough ness but of finite peak-to-valley amplitude δ_1–δ_2. This rules out the paradoxical limit of zero resistance, but does not remove the possibility that a flat surface with some roughness could reach the limit conductance of the perfect contact (which if the surface extends to infinity means perfect i.e. infinite conductance). This shows why results at large pressures (where the roughness could be nearly all compressed) may vary largely between various realizations depending on the features of the surface which make the roughness squeezed.

Interpretation of classical results using the GW model (Greenwood and Williamson, 1966) and its developments can be discussed in terms of conductance because of the analogy (2, 3). Suppose an exponential distribution of asperity summit heights $\phi(z_s) = (c/\sigma_s)\exp(-z_s/\sigma_s)$ where c is a arbitrary constant and σ_s is an amplitude parameter of the asperities summit height distribution. The total load is obtained by summing for all the asperities whose height z_s exceeds the separation d which will be compressed by the difference between z and d. Thus,

$$P = cN\exp(-d/\sigma_s)I_g \tag{4}$$

where the integral I_g is independent of the separation d, is dependent only on the deformation mode of the asperity, and N is the number of asperities per unit area. Hence, by using the analogy result (2) and differentiation of (4), it is trivial to show that the electrical conductance is linear with respect to total load

$$C_{GW} = \frac{2}{\rho E}\frac{P}{\sigma_s} \tag{5}$$

showing that the only asperity feature which seems to matter for the electrical conductance is the parameter σ_s, which is the analogous to the standard deviation in the Gaussian distribution. The height parameters are not very sensible to resolution even in the limit case of fractals when all the wavelengths are included, therefore the relation (5) is rapidly convergent showing that conductance is only affected by largest wavelength components of roughness. Of course, if the load is predicted from (4), this may be varying with resolution, because the asperity density N and the asperity radius which enters in the integral I_g are most likely affected by resolution.

Asperity theories are strongly limited in that they neglect interaction effects (and hence clustering effects of the conductance), and because of the disturbing result that the peak density goes as $1/(3\Delta) - 1/(4\Delta)$, where Δ is sampling interval – i.e. (Greenwood and Wu, 2001) "between 1 in 3 and 1 in 4 of all sample points is a peak!". This puts some worries about the definition of asperity based on 3-points peak local maxima of profile scans, and alternative definitions of asperity have been put forward.

In the light of these limitations, in this paper we shall not make use of asperity theories but of full solution of contact problems. However, we expect that at low loads the simplest asperity model result of linearity

between conductance and load (and modest influence of the roughness amplitude parameter only) could be confirmed, at least qualitatively, even by more refined investigations. This paper has of course some limitations: we use linear elasticity, and hence neglect plasticity. Also we assume plane profiles rather than full surfaces. Finally, we assume a periodic contact, and hence, the theoretical limit is infinite conductance. In practice, there will be a finite size of the specimen, leading to some "full contact" limit value of finite conductance.

2. The mechanics of contact of the Weierstrass profile

A much used description of fractal profiles is the Weierstrass series (Majumdar and Bhushan, 1991; Greenwood and Wu, 2001; Ciavarella et al., 2000, 2004a,b,c)

$$W(x) = g_0 \sum_{i=0}^{\infty} \gamma^{(D-2)i} \cos(q_0 \gamma^i x + \phi_i) \tag{6}$$

where g_0 is the amplitude of the first sinusoid, $q_0 = \frac{2\pi}{\lambda_0}$ is the circular frequency given by the wavelength of the first sinusoid, λ_0, and γ is a parameter (sometimes chosen to be 1.5 to have a non-periodic profile, but here chosen to be 2 for simplicity to have periodic functions). Finally, ϕ_n are random phases (not strictly needed for the Weierstrass series to be a fractal). The Weierstrass series used for generating profiles in numerical simulations are generally truncated to a number of terms n, the fractal limit obviously pertains to the asymptotic limit of n going to infinity. In the next figure there are any examples of fractal profiles with different γ (Fig. 3).

This function clearly has a discrete spectrum, and moreover shows approximate self-affine behavior, because of the first term. However, its spectrum can be approximated with a continuous power law PSD (Power Spectrum Density) function, and using the Sayles and Thomas notation (1978), at large frequencies we can write $G(\omega) = B\omega^{\beta}$, where B is a scale parameter of dimensions of length, and $-3 < \beta < -1$ is topothesy, related to fractal dimensions in the Mandelbrot terminology, as $D = 2.5 + \beta/2$. Here, we indicate by $1 < D < 2$ the fractal dimension of a profile.

The zeroth, second and fourth order moments of the PSD are known to be the variance of heights, slopes and curvatures, respectively, and are obtained by integrating over a pass-band of profile frequencies between a high-pass cutoff ω_H and a low-pass cutoff ω_L. For the power–law $G(\omega) = B\omega^{\beta}$, we obtain

$$m_0 \cong \frac{-B}{\beta+1}\omega_H^{\beta+1} \approx \frac{1}{L^{\beta+1}} = \frac{1}{L^{2D-4}}; \quad \text{and} \quad m_2 = \frac{-B}{\beta+3}\omega_L^{\beta+3} \approx \frac{1}{(\Delta)^{\beta+3}} = \frac{1}{(\Delta)^{2D-2}} \tag{7}$$

where Δ is a sampling interval, $\omega_L = 2\pi/\Delta$ and $\omega_L \gg \omega_H = 2\pi/L$. Here, L is the length of the profile scan. In other words m_0 depends only (modestly) on the length of the specimen. The slopes and curvatures are (nearly) independent of the high-pass cutoff but depend strongly on the sampling interval. So, Eq. (7) are important

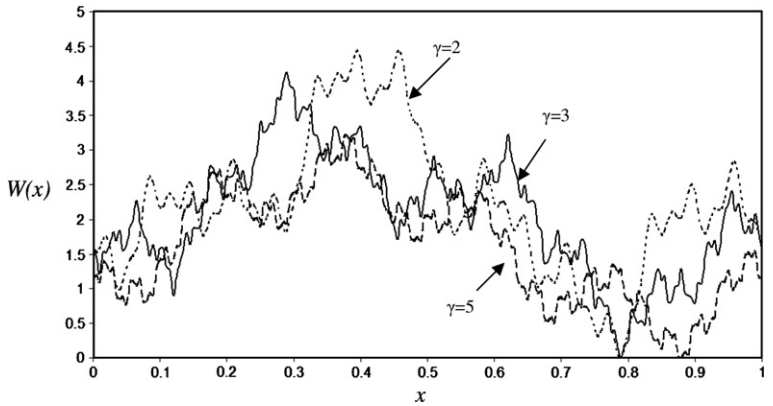

Fig. 3. Fractal profiles described by Weierstrass series for different γ (phases are random).

because they show the dependence of the moments of the sample length and interval and cutoff. Hence, for a series with n terms, it is found that

$$m_{0,W} = \langle W^2(x) \rangle = \frac{1}{2}(g_0)^2 \sum_{i=0}^{n} \gamma^{2(D-2)i}; \quad m_{2,W} = \langle W'^2(x) \rangle = 2\left(\pi \frac{g_0}{\lambda_0}\right)^2 \sum_{i=0}^{n} \gamma^{2(D-1)i} \tag{8}$$

The corresponding full contact pressure is given by superposition of the single sinusoid solution (Johnson, 1985, 13.2), which assuming zero mean pressure

$$p_{fc}(x) = (E^* q_0 g_0/2) \sum_{i=0}^{n} \gamma^{(D-2)i} \cos(q_0 \gamma^i x + \phi_i) \tag{9}$$

It is well known (Manners, 2000; Johnson, 1985, 13.3), the variance of full contact pressure is proportional to the variance of slopes $\sigma_w^p = \sqrt{m_{2,W}} = \sqrt{\langle W'^2(x) \rangle}$,

$$\left\langle p_{fc}^2(x) \right\rangle = \frac{1}{4} E^2 m_{2,W} = \frac{1}{2}\left(\frac{E q_0 g_0}{2}\right)^2 \sum_{i=0}^{n} \gamma^{2(D-1)i} \tag{10}$$

which makes it arguable that it is not possible to make "full" contact with any finite applied load. More specifically, in the deterministic version of the Weierstrass series (i.e. Eq. (6) without random phases), it is obvious that the full contact pressure (9) also does not depend on phases and hence there is no finite load to achieve full contact since the series does not converge (Ciavarella et al., 2000). However, this does not imply immediately that also infinite conductance is ruled out, since in principle, at least if we neglect interaction effects, perfect electrical contact is possible for contact over only part of the surface (Jang and Barber, 2003). We shall discuss this further in the results paragraph.

It can be shown that even an accurate elastic solution (at least in the limit of large γ) leads to a contact area which is a nearly linear function of load but with the coefficient is decreasing with the number of terms in the series. In fact, if we write dimensionless pressure $\tilde{p} = p/p^*$, where $p^* = E^* q_0 g_0/2$ is the full contact pressure of the first term, the decrease of contact area from A_0, the area of the first scale in contact for $n = 0$, is given by Ciavarella et al. (2000) *in the Hertzian regime* ($\tilde{p} < 0.2$) for large n, or large γ, by

$$A_n/A_0 = K_\infty \tilde{p} \gamma^{-(D-1)(n-1)} \tag{11}$$

with $K_\infty = 0.39139$.

In Fig. 4 we plot the dimensionless parameters $\tilde{\sigma}_w = \sqrt{m_{0,W}}/g_0$, and $\tilde{\sigma}_w^p = \sqrt{m_{2,W}}/\frac{g_0}{\lambda_0}$ from the two Eq. (8), the second of which in a log scale, as a function of the number of terms N included in the series. Notice that since $\gamma = 2$, the largest value $n = 10$ corresponds to $2^{10} = 1024$ smaller wavelength than the first term. Also, this is equivalent to have an ideal full profile, but changing the "sampling interval" which we can imagine using for measuring a Weierstrass series. For the *height parameter* σ_w the convergence is very rapid, with 4 terms in the series the values being very close to the converged values for $D = 1.25$, 6 terms for $D = 1.5$ and about all 10 terms for $D = 1.75$. Even for the large fractal dimension of $D = 1.75$, the difference between the value for a single sinusoid, and the converged value is only a factor 2. Different behavior, as expected, is obtained for the slopes parameter $\tilde{\sigma}_w^p$ which grows in a power–law, and increases of up to more than 2 orders of magnitude in the case of $D = 1.75$.

3. Weierstrass profile and the non-linear layer algorithm

In previous papers (Ciavarella et al., 2004a,b,c) we studied the conductance of the Weierstrass profile, *by keeping the assumption of large enough* γ. A full direct numerical algorithm was developed, and with other possible (simpler) approximations. The most accurate and efficient approximation was obtained with the non-linear layer model which will be here described shortly (a more complete description is in Ciavarella et al., 2004c). In terms of compliance, the non-linear method was seen to work only for $\gamma > 5$ which is not realistic for actual rough surfaces of engineering interest. Vice versa, no precise test was conducted in terms of conductance only for lower γ for which there is a need to consider random phases, and results are then interpreted in terms of mean values. A systematic investigation was not attempted, but as it will be shown in this paper, the non-linear

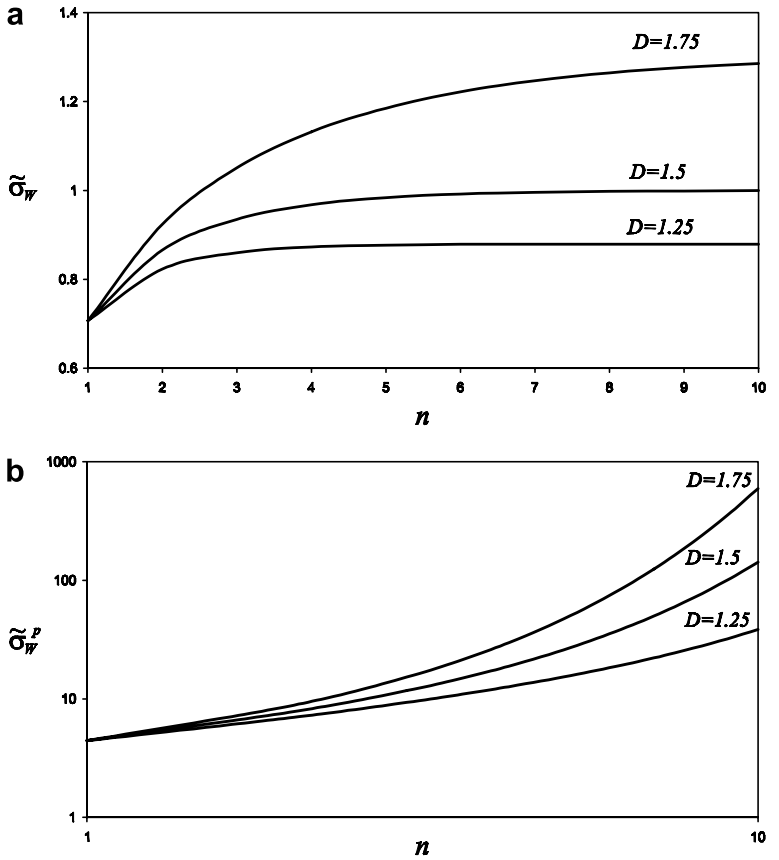

Fig. 4. The dimensionless parameters $\tilde{\sigma}_w = \sqrt{m_{0,W}}/g_0$, and $\tilde{\sigma}_w^p = \sqrt{m_{2,W}}/\frac{g_0}{\lambda_0}$ (see Eq. (8)), respectively, for (a and b), as a function of the number of terms n of a Weierstrass series with $\gamma = 2$. The 3 lines correspond to $D = 1.25$, 1.5, 1.75.

layer is much more efficient in terms of conductance than in terms of compliance and hence can in fact be used also for lower γ, *down to about 2*. The results will then be conveniently interpreted in terms of general trends.

The non-linear method can start from the smallest wavelength and going up in the scale. The first layer stiffness can be actually found analytically. Specifically, for a single sine wave of amplitude g, and wavelength λ, the relation between the approach δ and the mean pressure p is given by Ciavarella et al. (2004a), Eq. (17), obtained from the Westergaard solution by removing the term corresponding to the uniaxial uniform compression,

$$\frac{\delta}{g} = \tilde{p}[1 - \ln \tilde{p}] \tag{12}$$

A further quantity of interest is the electrical constriction resistance. Using Barber's analogy (2), the electrical contact conductance C is

$$C = -\frac{2}{\rho E}\frac{\mathrm{d}(pA_n)}{\mathrm{d}\delta} \tag{13}$$

and a *specific* conductance is obtained for unit area $A_n = 1$

$$C_s = \frac{C}{A_n} = -\frac{2}{\rho E}\frac{\mathrm{d}p}{\mathrm{d}\delta} \tag{14}$$

From Eq. (14) we can evaluate the analytical expression for the dimensionless conductance of a single sine wave, which results

$$\tilde{C} = -\frac{1}{\ln(\tilde{p})} \tag{15}$$

where $\tilde{C}$ is the *specific dimensionless conductance* given by

$$\tilde{C} = \frac{CE\rho}{2p^* A_n} \tag{16}$$

The idea of the non-linear layer approximation is to separate various components of roughness (extending the old idea of ''form'', ''waviness'' and ''roughness''), and in particular treating the microscopic roughness as a local non-linear spring acting on the macroscopic shape of the contact. The behavior of the system is then given by the combination of the stiffness of the large macroscopic punch with the local one of the small sinusoid. The local stiffness is not a constant but depends on the mean pressure applied on it. The problem becomes equivalent to the contact of two linear elastic bodies separated by a non-linear Winkler foundation.

During the contact process, when the indenter proceeds, the distribution of pressure on the single elements i of the contact area varies and accordingly also the stiffness K_i of the small springs varies. Because of the nature of the Winkler model, in which the degree of freedoms are uncoupled, the compliance matrix obtained for the layer is a diagonal one, and the effect of the springs is easily included. This procedure is iterated, i.e. the pressure distribution will be recalculated and so on till the results will converge using the 'consistency condition' as boundary condition – in other words, since the contact area is connected, it is possible to solve the problem for a given contact area (which makes the problem linear). This is a first advantage of the method, but an even greater advantage is that it can clearly be adapted to solve recursively multiscale rough profiles, instead of the full solution of the multiscale problem. In short, the linearized problem is solved and the contact area remains always mono-connected, since only the non-linear layer stiffness changes upon increasing of the number of terms simulated by the layer.

Hence, each 2-scale problem can be treated with more than sufficient accuracy with 100 elements, whereas to have the same accuracy with the direct method we need 100 elements for the smallest wavelength included in the model, and for a Weierstrass with 5 terms and $\gamma = 2$, this means 3200 elements. Finally, last but not least, a further very large advantage of the method is that the non-linear layer method implicitly ''produces'' the average results over random phases. In fact, a single stiffness result is obtained since the reduction to point wise springs makes the effect of phase irrelevant, and numerical experiments show that the resulting stiffness is very close to the *mean stiffness (averaging over random phases)*. In order to have the mean from direct simulation, the direct code with the large number of elements needs to run several times, and the advantage becomes evident. In practice, the non-linear method can give the converged result (i.e. the limit stiffness with an arbitrary number of terms) within a matter of minutes in our PC code implemented in MathCAD, whereas the full direct simulation takes hours to run the largest models we have attempted with 1600 elements.

4. Validation of the non-linear layer algorithm

Fig. 5 shows comparison of the non-linear layer method with full direct simulations, for $\gamma = 2, 3, 5$. The analytical result for the single sinusoid (Eq. (15)) is included for comparative purposes. Also, a linear approximation of the single sinusoid case is included as the chained dot line, which will be described later on, in Eq. (20). It is seen that the results of the non-linear layer are certainly excellent for $\gamma = 3$ *or greater*, satisfactory up to the $\gamma = 2$ *limit case.* Naturally, some degree of error is evident in the figures for the limit case $\gamma = 2$, but notice that for large $\tilde{C}$ even the mean of the full direct numerical simulations is prone to errors, since it is obtained starting from a numerical differentiation of the pressure-compliance curve which introduces systematic errors.

Hence, the non-linear layer algorithm is used with the following analysis with various values of D, γ, and n. Incidentally, for $\gamma < 2$, the non-linear layer method is seen to depart significantly from the results of the mean of the direct algorithm (figures are not included for brevity), but the case is not necessarily of interest (the Weierstrass series becomes aperiodic and further complications arise) (Fig. 6).

5. Results

In Fig. 7 we present the results for the specific dimensionless conductance. The analytical results for $n = 1$ is obtained from Eq. (15), while the values for $n = 2, 3, 4, 5, 6$ are obtained using the non-linear layer theory. Notice that the conductance is multiplied by the dimensionless rms amplitude factor

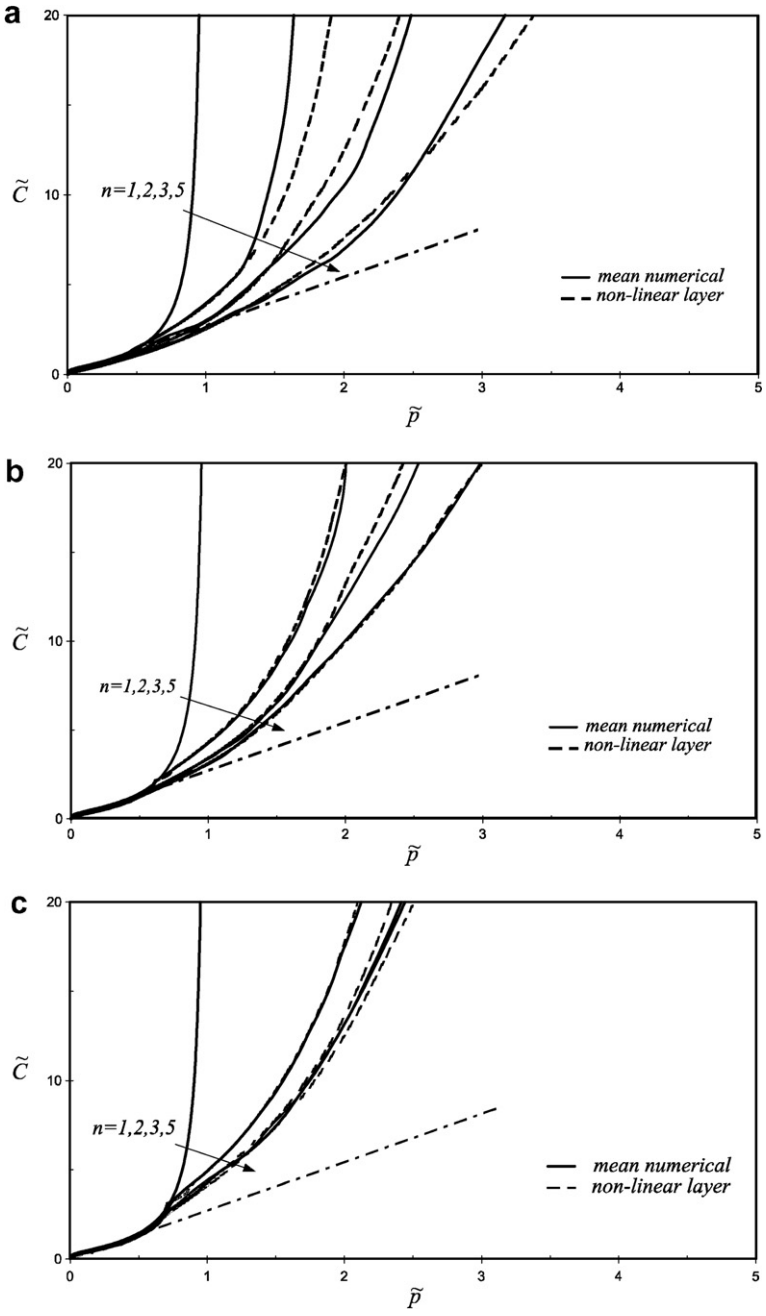

Fig. 5. Dimensionless specific conductance $\tilde{C}$ for $D = 1.5$. Comparison of non-linear layer and mean value of direct simulations, for $n = 2, 3, 5$. (a) $\gamma = 2$ and (b) $\gamma = 3$ and (c) $\gamma = 5$. The dash dot line $\tilde{C} = e\tilde{p}$ is the tangent to the conductance for the single sinusoid as it can be obtained from Eq. (20).

$$\tilde{\sigma}_w = \sqrt{m_{0,W}}/g_0 = \frac{1}{\sqrt{2}}\sqrt{\sum_{i=0}^{n}\gamma^{2(D-2)i}} \tag{17}$$

which is the ratio plotted in Fig. 4a, i.e. the ratio of the true SD of heights for each corresponding case, to the amplitude of the first term, g_0, so as to collapse all curves qualitatively in agreement to the GW asperity model result (5). In the following, we shall use this notation for dimensionless plots.

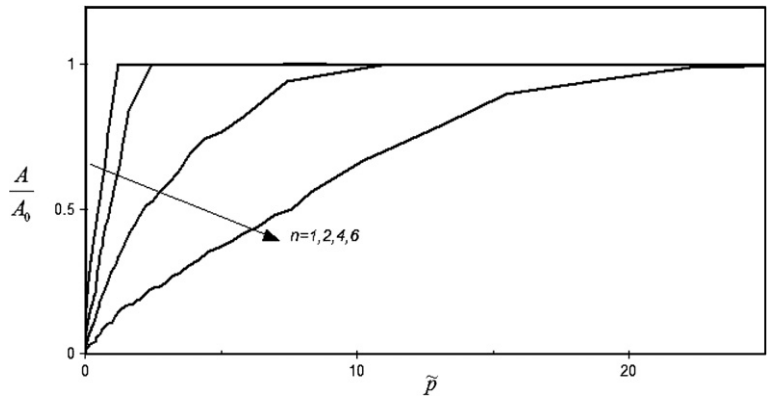

Fig. 6. Dimensionless contact area for $\gamma = 2$, $D = 1.75$ and various number of terms $n = 1, 2, 4, 6$.

Convergence is found apparently to a *limit curve*, particularly for low D (see Fig. 7a), where 4 waves give already the converged value at least in the range of pressures plotted. However, the question is to try to understand if this apparent convergence depends on the window chosen for the dimensionless pressure and conductance, or if we were to enlarge the window at larger pressures, no complete convergence would be found. This recalls the discussion on the introduction of this paper, and particularly appropriate is the work in progress by Manners and Gholami (2005). This in fact shows that it is possible that *conductance goes to infinity* with patterns of uniform contacts reducing in size at each stage of the process, but with gap sizes also tending to zero. In the most likely situation is that contacts pattern are generated by some kind of clustered model, similar to the 'Cantor Dust' model, *the gaps remain finite*, and the conductance also *remains finite*. Notice that this is already paradoxical, since it would not be immediate to expect zero contact area transmitting a finite amount of current! Notice that also Jang and Barber (2003) find convergence to perfect contact (i.e. infinite conductance) without full contact, but this is obtained neglecting interaction effects in $3D$, and hence is due to a very large number of contacts.

On some aspects of these theoretical questions, numerical experiments in a sense do not provide definitive answers, but our results do seem to converge to some forms increasing power–law exponent (i.e. increasingly slope in the log–log plots), and hence even though there may never be "perfect" contact, this in practice is found for finite pressures, without full contact. On the contrary, we know that the contact area seems to decrease without limit upon increase of the number of terms, as shown in Fig. 7 in an example case, and suggested by the approximate results in Ciavarella et al. (2000) in Eq. (11). Hence, for a given applied pressure, while the conductance tends to not change after a few terms, the contact area certainly continues to decrease.

Hence, the convergence of the macroscopic conductance is eventually entirely due to the parallel of an infinite number of infinitesimal contact areas, whose interaction has to be included as otherwise the conductance does not converge (Jang and Barber, 2003). The even more paradoxical result to find an infinite conductance for a zero contact area does seem less probable since we would need to produce contact uniformly everywhere, according to Manners and Gholami (2005), and this is ruled out by the presence of the first terms of the series which produce gaps in certain regions which are never reattached in contact in the solution with more terms in the series.

One of the most interesting aspects is that linearity is *not* found as expected from asperities theories. This may be due to the fact that we are considering two-dimensional profiles, but consider the conductance in the low-pressure regimes of the single sinusoid case: despite the logarithmic singularity near the origin, the conductance in (15) is approximately linear. More precisely, taking the product $\tilde{C}\tilde{\sigma}$ for the single sinusoid, which from Eqs. (15) and (17) is

$$\tilde{C}\tilde{\sigma} = -\frac{1/\sqrt{2}}{\ln(\tilde{p})} \tag{18}$$

its derivative being

$$\frac{\delta\tilde{C}\tilde{\sigma}}{\delta\tilde{p}} = \frac{1/\sqrt{2}}{\tilde{p}\ln^2(\tilde{p})} \tag{19}$$

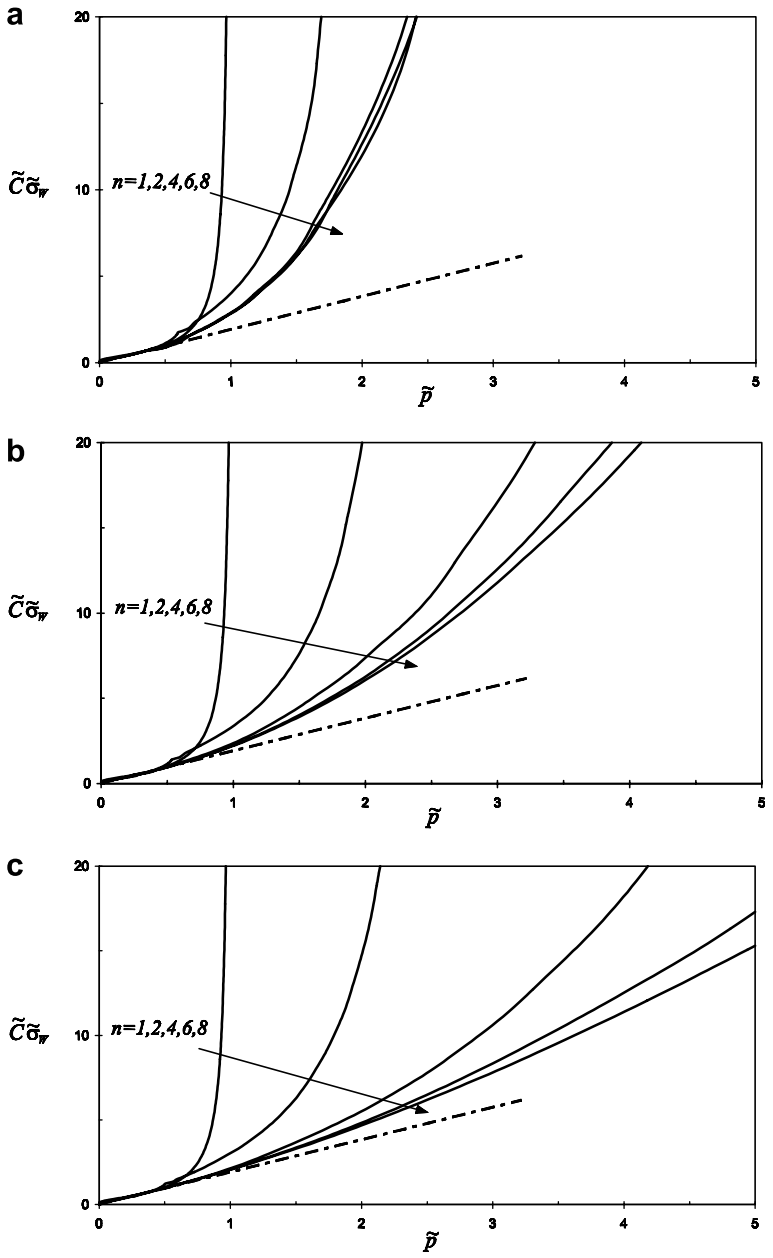

Fig. 7. Dimensionless specific conductance $\tilde{C}\tilde{\sigma}_w$ for $\gamma = 2$ and various number of terms $n = 1, 2, 4, 6, 8$ (a) $D = 1.05$, (b) $D = 1.5$, (c) $D = 1.75$. The dot dash line is defined in Eq. (20).

we notice that at $\tilde{p} = 1/e$ (where e is the base of natural logarithms) the derivative is $e/\sqrt{2}$ and hence the line $\tilde{C}\tilde{\sigma} = e\tilde{p}/\sqrt{2}$ is tangent to the correct curve (18), goes to the origin, and approximates reasonably well the intermediate range of pressures (e.g. in the range $\tilde{p} = 0.2 - 0.6$). For more general profiles, also because of the asperity model results, we would expect some deviations due to logarithmic terms, but above a given threshold of pressure, a linear relationship should emerge such as

$$\tilde{C} = \frac{e}{\sqrt{2}} \frac{\tilde{p}}{\tilde{\sigma}_w} \tag{20}$$

where the denominator actually depends on the number of terms and the fractal dimension (17).

Fig. 7 shows the variation of conductance for $D = 1.05$, 1.5 and 1.75, along with the linear approximation of Eq. (20). It is clear that increased agreement with the linear law (20) is found with respect to the case of the single sinusoid. However, this is more true for the large D case than for the low D case, where the linear behavior remains limited in terms of pressure range.

Fig. 8 shows the variation of conductance for different γ: $\gamma = 3, 5, 10$ instead of 2 as in Fig. 7. When γ increases, the conductance converges much faster with the number of waves (but this is expected, since the range of wavelengths changes much faster with n when is γ is larger). However, the tendency to linearity is further reduced with respect to the case of low γ, and "knee points" appear. This result is also expected, because for larger γ the effect of higher order terms in the series is reduced.

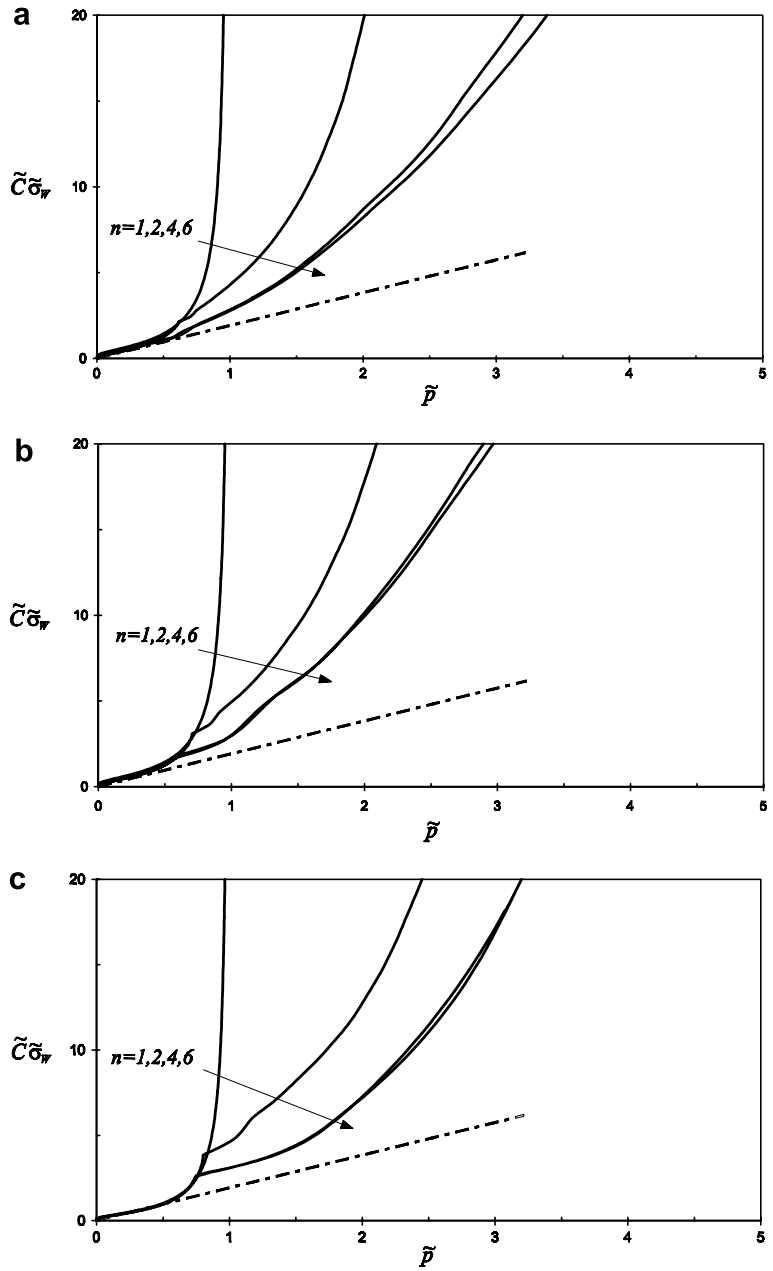

Fig. 8. Dimensionless specific conductance $\tilde{C}\tilde{\sigma}_w$ for $D = 1.5$ and various number of terms (a) $\gamma = 3$, (b) $\gamma = 5$, (c) $\gamma = 10$. The dot dash line is the linear approximation of Eq. (20).

6. Possible fitting equations

Results so far have been given in semi-log plots for convenience. In order to return to the original discussion of the experimental results in Fig. 1, the next Fig. 9 gives the dimensionless conductance with a high number of terms (specifically for $n = 6$) as a function of the dimensionless pressure in a log–log graph, and with a large range of values spanning 5 orders of magnitude in the x-axis and 6 orders of magnitude on the y-axis (there were only 3 orders of magnitude for both x- and y-axis in the original Fig. 1). It can be first observed that all results lye between the single sinusoid results (Eq. (18)) and the linear law (Eq. (20)). Second, the results seem not to depend significantly on fractal dimension in a first region, and then a continuous increase of the slope is seen, which is more evident for low fractal dimensions. Hence, we attempted fitting the results here obtained by the sum of two distinct power laws. In particular, the best fit power law exponent obtained is 2/3 in the first regime, and the power law becomes very close to the exponent $3/D$.

Hence, a resulting possible law is

$$\tilde{C}\tilde{\sigma}_{\mathrm{w}} = \tilde{p}^{2/3} + \tilde{p}^{3/D} \tag{21}$$

and the approximation (at least within the collapse inherent to the log–log plot with such wide range of results) seems to be quite good. Notice that there is a significantly extended ''transition regime'' well represented by the linear approximation of Eq. (20). A re analysis of Fig. 1 shows that the experimental trends, although largely variable, seem to be simply power laws or display asymptotic power laws at the ends, with only one exception. The comparison of the results obtained with the theoretical electrical conductance of the first scale single wave suggests that if the roughness of a real surface is due prevalently to a single wave, the behavior differs significantly from a power law, with an apparent local lower exponent in the low-pressure regime and with a quick raise to infinity when the pressure leads to the complete contact. This is a further way to explain some behaviors observed in Fig. 1. The present numerical would not change significantly if a larger n were to be used than the $n = 6$ used here, except perhaps at the very large pressures. Notice however that the case we are considering corresponds to an infinite extension of the specimen, whereas in practice finite size of the specimen will give a finite limit to the conductance, and hence another regime will be added, which corresponds to a ''plateau'' in the conductance, with a transition region which may give opposite curvature and result finally in a sigmoidal shape as it is observed in some of the curves in Fig. 1.

Finally, in Fig. 10 we trace dimensionless conductance for different $\gamma = 2, 3, 5, 10$ and high number of terms n. We find surprisingly close results, even for the largest $\gamma = 10$, smaller than we were expecting, suggesting that for profiles having the same approximate PSD (since different γ only correspond to different approximations

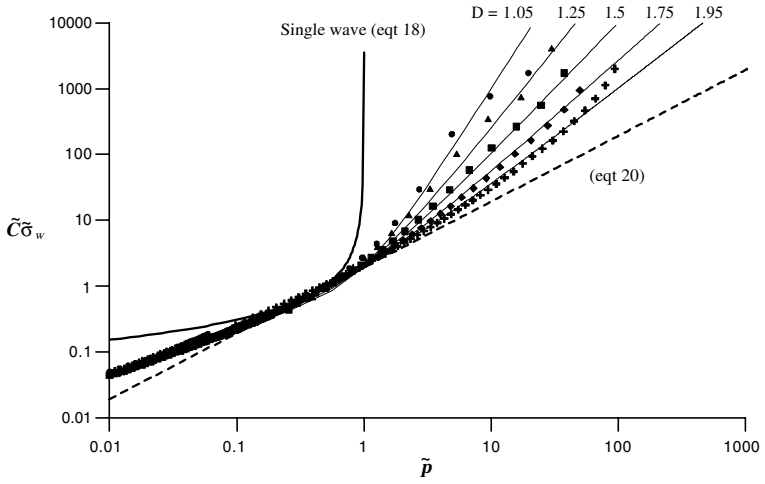

Fig. 9. Dimensionless specific conductance, for $\gamma = 2$, $n = 6$ and different D. The symbols are the numerical results. The thin solid lines are the fitting function (21) for the different fractal dimension. For a complete comparison the single wave defined in Eq. (18) and the dash dot line is the linear approximation of Eq. (20) are introduced.

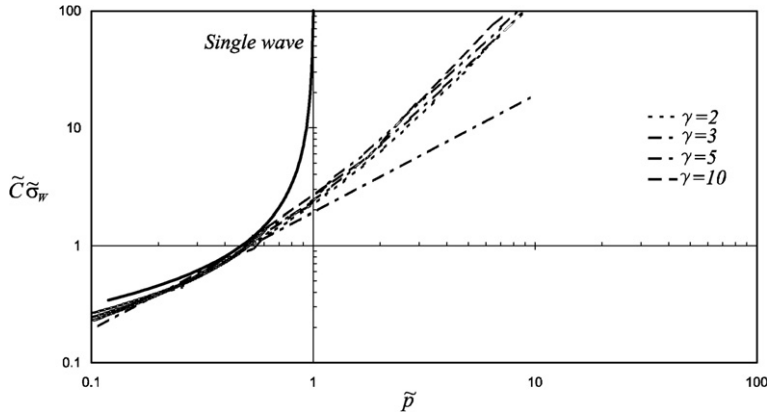

Fig. 10. $\tilde{C}\tilde{\sigma}_w$ for $D = 1.5$, $n = 6$ and different $\gamma = 2, 3, 5, 10$. The dot dash line (Eq. (20)) is the tangent to the curve (Eq. (18)).

of the same power–law PSD), approximately the same results are obtained in terms of conductance. Notice that this does not mean that the Archard approximation, described in Ciavarella et al. (2004b) works here, as numerical comparisons show that the latter only works for extremely large γ, i.e. of the order of 50 or greater. As it is clear from Fig. 8, however, some deviations do occur, since for high γ the effect of further terms tend to be "separated" from the previous terms, and hence the conductance curve tends to present "knee points" and be less continuous. Hence, the effect of "texture" of roughness is far from trivial, and gives rise to a range of possible behavior.

7. Conclusions

Using an ad hoc developed approximate numerical procedures for the solution of a line contact problem which is competitive to obtaining the mean results with several runs of a full direct numerical solution code, we have studied the problem of conductance of multiscale roughness profiles. The results show:

(1) the strong dependence on the random phases indicates that results may show considerable scatter from one specimen to another;
(2) the inverse dependence on the RMS amplitude of the profile roughness, like expected from asperities theory of Greenwood and Williamson;
(3) a less-than-linear behavior at low pressures, with a possible power–law with exponent less than 1 and in particular close to 2/3;
(4) dominance of the first few terms of the series at low pressures, but higher order terms being important only at higher and higher pressures;
(5) a transition regime for intermediate levels of dimensionless pressures, which can be approximated to linear;
(6) dependence on the fractal dimension at higher pressures, with increase more than linear particularly at low D.

The patterns obtained seem to explain some of the trends evidenced in Fig. 1 and hence helps in shedding more light in the apparent controversial question on the effect of roughness in the conductance of rough surfaces. In particular, since roughness tends to be squeezed out, the trends we see show conductance tends to increase more than linearly (particularly at small fractal dimensions). However, another limit could be found in terms of the finite size of the specimen, which may suggest a transition towards reaching a finite limit. The resulting curves could then be sigmoidal, as confirmed by qualitative comparisons with experiments in the literature, where roughness seems to produce large difference in quantitative and qualitative terms, the former differences being due mainly to amplitude or roughness, and the second to the texture parameters.

Acknowledgments

We acknowledge funding for the European project AUTOCON. Integrated Wiring and Interconnecting of Electrical and Electronic Components for "Intelligent" Systems, Contract Number: G1RD-CT2001-00588.

References

Archard, J.F., 1957. Elastic deformation and the laws of friction. Proc. R. Soc. Lond. A 243, 190–205.
Barber, J.R., 2003. Bounds on the electrical resistance between contacting elastic rough bodies. Proc. R. Soc. Lond. A 459, 53–66.
Bush, A.W., Gibson, R.D., Thomas, T.R., 1975. The elastic contact of a rough surface. Wear 35, 87–111.
Ciavarella, M., Demelio, G., Barber, J.R., Jang, Y.H., 2000. Linear elastic contact of the Weierstrass profile. Proc. R. Soc. Lond. A 456 (1994), 387–405.
Ciavarella, M., Murolo, G., Demelio, G., Barber, J.R., 2004a. Elastic contact stiffness and contact resistance for the Weierstrass profile. J. Mech. Phys. Solids 52 (6), 1247–1265.
Ciavarella, M., Murolo, G., Demelio, G., 2004b. The electrical/thermal conductance of rough surfaces, the Weierstrass–Archard multiscale model. Int. J. Solids Struct. 41, 4107–4120.
Ciavarella, M., Demelio, G., Murolo, G., 2004c. A numerical algorithm for the solution of 2D rough contact problems. J.Strain Anal. Eng. Des. 40 (5), 463–476.
Greenwood, J.A., Williamson, J.B.P., 1966. The contact of nominally flat surfaces. Proc. R. Soc. Lond. A 295, 300–319.
Greenwood, J.A., Wu, J.J., 2001. Surface roughness and contact: an apology. Meccanica 36 (6), 617–630.
Holm, R., 1958. Electric Contact, Theory and Application. Springer-Verlag, Berlin (Germany).
Jang, Y.H., Barber, J.R., 2003. Effect of contact statistics on electrical contact resistance. J. Appl. Phys. 94 (11), 7215–7221.
Johnson, K.L., 1985. Contact Mechanics. Cambridge University Press, Cambridge (UK).
Majumdar, A., Bhushan, B., 1991. Fractal model of elastic–plastic contact between rough surfaces. ASME J. Tribol. 113, 1–11.
Mandelbrot, B., 1982. The Fractal Geometry of Nature. W.H. Freeman, San Francisco.
Manners, W., 2000. Heat conduction through irregularly spaced plane strip contacts. Proc. Inst. Mech. Eng. C J. Mech. Eng. Sci. 214 (C8), 1049–1057.
Manners, W., Gholami, B., 2005. Private communication of a preprint paper "Constriction Resistance Between Materials with Fractal Patterns of Contact".
Sayles, R.S., Thomas, T.R., 1978. Surface topography as a nonstationary random process. Nature 271, 431–434.
Snaith, B., O'Callaghan, W., Probert, S.D., 1983. Can standards be set for reliable measurements of thermal contact conductance? In: AIAA 21st Aerospace Science Meeting Reno Nevada, Paper 83-0533.
Whitehouse, D.J., Archard, J.F., 1970. The properties of random surfaces of significance in their contact. Proc. R. Soc. Lond. A, 97–121.